The measurement of aerosol optical properties at a rural site in Northern China

P. Yan, J. Tang, J. Huang, J. T. Mao, X. J. Zhou, Q. Liu, Z. F. Wang, H. G. Zhou

Atmos. Chem. Phys. Discuss., 7, 13001–13033, 2007
www.atmos-chem-phys-discuss.net/7/13001/2007/

Atmospheric Chemistry and Physics Discussions

The measurement of aerosol optical properties at a rural site in Northern China

P. Yan[1], J. Tang[1], J. Huang[3], J. T. Mao[2], X. J. Zhou[1], Q. Liu[4], Z. F. Wang[4], and H. G. Zhou[4]

[1]Chinese Academy of Meteorological Sciences of CMA, Beijing, China
[2]Atmospheric Department, Peking University, Beijing, China
[3]Guangzhou tropical meteorological institute of CMA, Guangzhou, China
[4]Beijing meteorological Bureau, Beijing, China

Received: 15 June 2007 – Accepted: 25 July 2007 – Published: 6 September 2007

Correspondence to: P. Yan (yanpeng@cams.cma.gov.cn)

Abstract

Atmospheric aerosols contribute one of the largest sources of uncertainty in the estimation of climate forcing. During the period from April 2003 to January 2005, in situ measurements of aerosol optical properties were conducted at a rural site in Northern China, Shangdianzi Global Atmosphere Watch (GAW) regional station (SDZ). Based on the daily average data, the means (standard deviation, S.D.) of scattering and absorption coefficients for the entire period were 174.6 Mm^{-1} (189.1 Mm^{-1}) and 17.5 Mm^{-1} (13.4 Mm^{-1}), respectively. These values were approximately one third of the reported values for scattering coefficients and one fifth of those for absorption coefficients obtained in the Beijing urban area. The mean single scattering albedo (SSA) for the entire period was 0.88 (0.05), which was about 0.07 higher than the values reported for the Beijing urban area, and also higher than the values (0.85) used in the climate model simulation for China and India. Both the absorption and scattering coefficients showed the lowest values in winter (11.2 Mm^{-1} and 128.9 Mm^{-1}, respectively), while the highest values appeared in summer for absorption coefficients (22.1 Mm^{-1}) and in fall for scattering coefficients (208.2 Mm^{-1}). The mean SSA were lowest in spring (0.85) and highest in winter (0.90). The daily variations of aerosol absorption and scattering coefficients were strongly influenced by synoptic changes throughout the observation period. A trajectory cluster analysis was applied to discern the source characteristics of aerosol optical properties for different air masses. The cluster mean scattering coefficients, absorption coefficients and SSA were all high when the air masses moved from SW and SE-E directions to the site and aerosols were influenced with heavy pollution from the dense population centers and industrial areas. The cluster mean SSA for air masses coming from the polluted areas was not only higher than those with the trajectories from the "clean" directions, but also higher than the reported values for the regions with high pollution emissions (such as Beijing urban area). This fact might reflect the substantial secondary aerosol production during the transport. The characteristics of aerosol optical properties measured at this rural site suggest the significant

ACPD

7, 13001–13033, 2007

impacts of human activities on the regional aerosol.

1 Introduction

Aerosols perturb the radiation balance of the Earth directly through scattering and absorbing solar radiation, and indirectly by acting as condensation nuclei in cloud formation, thus affecting the optical properties and lifetimes of clouds (Rosenfeld, 1999; Rosenfeld, 2000; Twomey, 1977). The optical properties of aerosols are related to both their chemical compositions and particle size distributions. Atmospheric aerosols in different regions consist of varying compositions and size modes, which lead to different radiative impacts on regional climate. Among them, black carbon (BC) aerosol is in particular important due to its strong light absorption in the terrestrial radiation balance and hydrological cycle (Jacobson, 2002; Menon et al., 2002; Ramanathan et al., 2001). As opposed to of the well mixed green house gases, the global distribution of aerosol is extremely inhomogeneous and the characterization of aerosols has so far been poorly parameterized in climate models (Anderson et al., 2003). The spatial and temporal variations of the radiative forcing by aerosols are strongly influenced by local variations of aerosol mass concentrations, size distributions and optical properties. For this reason, the characterizations of aerosol properties in various regions around the global are essential to the estimation of their climate impacts.

In China, as a result of the rapid population and economic growth, emissions of anthropogenic pollutants have increased dramatically. Studies revealed that emissions of SO_2 and NO_x in China were similar in magnitude with those of Europe and eastern North America (Akimoto and Narita, 1994), but aerosol sources in China have their unique features. The mixture of heavy air pollution from urbanization and industrial activities and the increases of desert dust particles result in the rather complex nature of aerosol optical properties in China (Holler et al., 2003). The high rate of usage of coal and biofuels and lower combustion efficiency has made China a significant source of BC. It was estimated that BC emitted in China accounted for roughly one-fourth

ACPD
7, 13001–13033, 2007

of the global anthropogenic emissions, though a significant uncertainty exists in the estimations of the submicron BC emission inventory (Cooke et al., 1999; Street et al., 2001). Uncertainties in the measurement of optical properties of aerosols in China and other Asian countries present one of the largest sources of uncertainty in the estimation of aerosol radiative forcing (Holler et al., 2003). In the past 20 years, many studies have focused on the mass concentrations and physical and chemical properties of aerosol in China, but only a few short term measurements were conducted focusing on aerosol radiative properties (Xu et al., 2004; Xu et al., 2002).

In this paper, a 21 month study of in situ measurements of aerosol properties at a rural site in northern China is presented, and the characteristics and variation of aerosol optical properties are reported. Filter analysis was performed to provide insight on the chemical composition of aerosols, and the influence of air mass transport on the optical properties of aerosol was determined through the trajectory clustering analysis.

2 The experiment

2.1 Site descriptions

Shangdianzi station (SDZ, 117°07′ E, 40°39′ N, 293.3 m a.s.l.) is located in Miyun County, a suburb of the Beijing metropolis. The site is on the gentle slope of a small hill. The geography surrounding the station is characterized by rolling hills with farmland, orchard and forests. On the foot of the hill about 2 km south is the Shangdianzi village with about 1200 inhabitants. The major local economical activities within Miyun County are farming and fruit growing. Since Miyun reservoir is the major water supply to the Beijing metropolitan area, Miyun County has been designated as a “Preserved Area”, which means that there are only minimal natural and anthropogenic pollution sources within a 30 km range surrounding the site.

Figure 1 shows the map of SDZ station and some cities or regions with dense population and high industrial activities. As the map indicates, the major sources of pollution

in this region are located predominantly west to southeast of the site. The regions in the northern sector are much less inhabited, comprised of the vast grassland of Inner Mongolia and mountainous rural regions of Hebei province, where the population is relatively sparse and industrial activities less prevalent.

2.2 Measurements and instrumentation

During the period from April 2003 to January 2005, an intensive study of aerosol optical properties was conducted at SDZ GAW station in Northern China. The experiment included the measurement of aerosol scattering and absorption coefficients, size-resolved aerosol mass and chemical compositions, and meteorological observations.

Table 1 lists the measured parameters and the instruments used in the experiment. The scattering coefficient of aerosol (σ_{sc}) was measured with Integrating Nephelometer (Model M9003, ECOTech, Australia). This instrument used LEDs as the light source at a wavelength of 525 nm. The scattering integration angle is from 10° to 170°. The truncation error correction was not applied to the data in the study since there was no dust storm during the entire observation period and the truncation errors are small for submicrometer aerosols. Theoretical estimation based on Mie-theory indicated that the truncation error was less than 10% for fine particles. A background (zero) check was done automatically by pumping in particle-free air once each day and a weekly span check was performed manually by the operator using particle-free HFC-R134a gas recommended by the manufacturer. The relative humidity (RH) in the cell of the instrument was controlled below 60% by an automatic heating inlet provided by the manufacturer. This heating inlet could cause evaporation of volatile species, such as nitrate and some volatile organic matter. Bergin et al. (1997) studied the decrease of scattering coefficient caused by the evaporation loss of aerosols in a nephelometer, and it was generally less than 20% for the pure nitrate aerosol, Therefore, the reduction of the measured aerosol scattering coefficient due to the heating of our inlet was expected to be much less because the nitrate accounted for only a small fraction of the total mass in fine particles in northern China (Zhang et al., 2003).

ACPD
7, 13001–13033, 2007

The BC aerosol concentration was measured with Aethalometer (Model AE31, Magee Scientific, USA). The AE31 Aethalometer measured the optical attenuation of light from LED lamps with seven different wavelengths (370, 470, 520, 590, 660, 880, and 950 nm) transmitted through the aerosols deposited continuously on a quartz fiber filter (Hansen et al., 1984). The difference in light transmission through the particle-laden sample spot and a particle free reference spot of the filter is attributed to the absorption caused by aerosol. The attenuation of light is converted to the BC mass concentration using wavelength dependent calibration factors as recommended by the manufacture (Manual of Aethalometer, Magee Scientific). As discussed below, the Aethalometer light attenuation measurement was used to calculate the aerosol light absorption coefficient (σ_{ab}).

All of the data of scattering and absorption coefficient and relevant ancillary parameters were recorded at 5 minute intervals. The datasets have been manually edited to remove invalid data resulting from instrumental or sampling problems.

The size-resolved aerosol filter sampling was made only for some specific time periods in each season. The analysis included mass concentrations and some of the major chemical compositions, such as ions, metals and organic and elemental carbons (OC and EC) of aerosols. The procedure for mass gravimetric and chemical analysis was identical to those described in the references (Bergin et al., 2001; Yan et al., 2006).

2.3 Method for absorption coefficient calculation

Light absorption coefficient can be directly calculated from the attenuation measured by Aethalometer or indirectly calculated based on the BC concentrations recorded by the instrument.

The direct calculation of light absorption at any wavelength uses the following formula (Bodhaine, 1995; Weingartner et al., 2003):

$$\sigma_{ab} = \frac{A}{Q} \times \frac{\Delta ATN}{\Delta t} \times \frac{1}{CR} \quad (1)$$

where,A is the filter spot area, Q the volumetric flow rate and ΔATN is the change in attenuation during the time interval Δt, and C is a wavelength independent empirical correction factor, which corrects for the enhancement of the optical path in the filter due to multiple scattering of the light beam at the filter fiber, R is the correction factor describing the changes in instrumental response with increased particle loading on the filter (shadowing effect). The C factor was found to vary with different aerosol types and mixing state, and R to be unity for aged particles (Weingartner et al., 2003).

The indirect way to obtain the light absorption coefficient from the recorded BC concentration is based on the following equation:

$$\sigma_{ab} = \alpha \times [BC] \quad (2)$$

where, α is the conversion factor or the BC absorption efficiency, which can be determined theoretically from Mie-theory or empirically from linear regression of the Aethalometer BC concentration data against the aerosol absorption coefficient measured from a reference method (Arnott et al., 2005; Arnott et al., 2003; Clarke and Charlson, 1985).

In this work, the indirect method (based on the recorded BC concentration by the Aethalometer) was accepted to calculate the aerosol light absorption coefficient. The conversion factor α was obtained based on the result of the intercomparison experiment conducted in southern China (Schmid et al., 2005). In that experiment, the conversion factor α=8.28 m^2/g (with correlation coefficient R^2=0.92) was derived by a linear regression of the BC concentrations at 880 nm (in the unit of $\mu g/m^3$) of Aethalometer against the light absorption coefficients at 532 nm (in units of Mm^{-1}) simultaneously measured with a photoaccoustic spectrometer (PAS). This conversion factor is comparable to ~8–10 m^2/g (at 550 nm) obtained in Mexico city (Barnard et al., 2005), but a little lower than the historical value of 10 m^2/g often accepted for urban aerosols (Moosmuller et al., 1998), and higher than the value of less than 7 m^2/g for diesel soot suggested by Fuller (Fuller et al., 1999). However, it was very close to the value of approximate 8.0 m^2/g obtained in Beijing urban area by Bergin (Bergin et al., 2001)

ACPD
7, 13001–13033, 2007

and that of 8.5 m^2/g reported by Arnott from BRAVO (Big Bend Regional Aerosol and Visibility Observation Study) (Arnott et al., 2003).

3 Results and discussion

3.1 Aerosol optical properties and BC concentrations

Figure 2 and Table 2 show the time series and the statistics of daily-average BC and aerosol optical properties measured during the experiment. The mean (S.D.) concentration of BC, absorption and scattering coefficient for the entire period were 2.12 $\mu g/m^3$ (1.62 $\mu g/m^3$), 17.54 Mm^{-1} (13.44 Mm^{-1}), and 174.6 Mm^{-1} (189.1 Mm^{-1}), and the median values were 1.78 $\mu g/m^3$, 14.71 Mm^{-1}, and 101.6 Mm^{-1}, respectively. It should be noted that the large standard deviation for each variable reflected the strong fluctuation of the measured aerosol properties.

On average, the absorption and scattering coefficient at SDZ were about one-fifth and one-third lower than those measured in the Beijing urban area in summer 1999, as listed in Table 3. The mean absorption coefficient at SDZ was comparable to those obtained at Lin'an regional background station in a rural area in the Yangtze Delta Region (Xu et al., 2002) and Cape D'Aguilar station of Hong Kong in eastern and southeastern China (Man and Shih, 2001), but higher than that measured at Yulin in Gobi Desert (Xu et al., 2004). The scattering coefficient at SDZ was only about half of that at Lin'an station, and much higher than that of Cape D'Aguilar (Man and Shih, 2001; Xu et al., 2002), but similar to that at Yulin in Gobi Desert (Xu et al., 2004).

The single scattering albedo (SSA) is defined as the ratio of aerosol scattering coefficient to the extinction coefficient (sum of the absorption and scattering coefficient). This parameter is especially important in the estimation of direct aerosol radiative forcing, since even small errors in its estimation might change the sign of aerosol radiative forcing (Takemura et al., 2002). To calculate SSA, a wavelength correction for aerosol absorption was applied to the measured absorption coefficients. The result showed

ACPD
7, 13001–13033, 2007

EGU

that the mean and the median value of SSA (at 525 nm) obtained at SDZ were 0.88 and 0.90, respectively (see Table 2). This mean SSA was within the range of 0.85–0.95 retrieved through AERONET for northern hemisphere (Dubovik et al., 2002), but lower than the value of 0.93 obtained at Lin'an in November, 1999 (Xu et al., 2002) and 0.95 at Yulin (Xu et al., 2004). It was about 0.07 higher than that (0.81) reported for the Beijing urban site (Bergin et al., 2001), and also higher than the value (0.85) used in the climate modeling for China and India simulations (Menon et al., 2002).

As with SDZ, Lin'an and Cape D'Aguilar can be considered to be the background sites in each economic/climate area in eastern China, and it could be inferred that the scattering coefficients of aerosols in eastern China are more variable than absorption coefficients, which reflect the different sources and formation processes of aerosols in these regions .

Compared to the results measured in Northern America (see Table 3), the mean absorption coefficient at SDZ was about three to four times greater than the mean value measured at Bondville, Illinois (BND), a rural location in the east central region of Unite States, and forty five times greater than that measured at Barrow, Alaska (BRW), a clean region in North America. The mean scattering coefficient was three times greater than that at BND and eighteen times greater than that measured at BRW, and the mean SSA was about 0.04 and 0.08 lower than the value of BND and BRW, respectively (Delene and Ogren, 2002).

3.2 Seasonal variations of aerosol optical properties

The seasonal variations (based on 24-h average) of absorption, scattering coefficient and SSA of aerosols for the entire observational period are presented in Table 4. It was found that the absorption coefficient was higher in summer and spring and lower in fall and winter with the highest in summer and the lowest in winter. The scattering coefficient showed a slightly different seasonal distribution. The scattering coefficients were elevated in fall and summer with the highest levels observed in fall and lower in winter and spring with the lowest levels in winter. Corresponding to the variation

of absorption and scattering coefficients, the calculated SSA values were higher in winter and fall, but relatively low in spring and summer. Sheridan et al. (2001) had reported similar seasonal variations of aerosol absorption coefficient at the Southern Great Plains Cloud and Radiation Testbed site (SGP CART site), where the light absorption coefficients were higher in the late spring through fall (April through fall), and also generally lower SSA values over the same time period were found. However, the seasonal variations of aerosol properties at SDZ were obviously different from those measured in Cape D'Aguilar of Hong Kong (see Table 2), where the highest values of absorption and scattering coefficients were found in winter and fall, and the lowest in summer (Man and Shih, 2001). The reasons for such seasonal variations at SDZ site are complicated, and include the seasonal changes in source emissions, atmospheric transport, and chemical transformations. The prevailing wind direction shifting over different seasons is probably one of the important factors, as indicated from wind rose plot of the site (Fig. 3).

In spring (from March to May, 2004), the dominant wind directions at SDZ site were WSW and SW winds, and as a consequence, the advection of the air masses from highly populated and polluted regions caused the enhancement of absorption and scattering coefficients at the site. In summer, although the frequency of wind from NE and ENE direction increased, a significant fraction of the winds still came from the WSW and SW. There was frequently the occurrence of crop residue burning after the harvest in this region, and the combination of transport and increased biomass combustion emissions caused the highest absorption coefficient in summer at the site. In winter, the prevailing wind shifted to ENE and NE, where there were no strong anthropogenic or combustion aerosol sources from these directions, and the clean air masses resulted in the lowest levels of the measured aerosols at the site. In fall, the frequency of the WSW wind direction decreased and the ENE wind increased, and as a result the mean absorption coefficients were lower in fall than in summer but higher than in winter.

In contrast to the aerosol absorption coefficient, however, the higher levels of scat-

tering coefficient in the fall could not be satisfactorily explained only by shifts in the prevailing wind. Another process that can enhance aerosol scattering coefficients is the chemical production of secondary aerosols, either through photochemical reactions or in fogs. The more frequent occurrence of fogs in the fall period was documented through meteorological observations indicating more foggy days and poor visibility at the site. Table 5 showed the number of days with fog and poor visual range in each month. There were 28 foggy days in the fall (September, October and November) of both years, with 3 heavy fog days in 2003 and 4 heavy fog days in 2004. Under the fog weather conditions the growth and/or heterogenic production of aerosol during transport could significantly enhance the scattering coefficient, as illustrated in the daily average dataset, the highest daily average aerosol scattering coefficients were often found on the heavy fog day in the fall in both years.

3.3 The Diurnal variations of measured aerosol optical properties

Figure 4 shows values of aerosol absorption, scattering coefficient, and SSA averaged for each hour of a day during the period from September 2003 to January 2005 as a function of local time. There were clear diurnal variations for all variables. For the absorption coefficient, the minimum values occurred in the early afternoon (around 13:00 p.m.), and the highest values were observed during the night, which reflects the turbulent dilution of the pollutants. The local maximum value of the absorption coefficient appeared in the morning (around 08:00 a.m.), which corresponds with local emissions of light absorbing material from human activities surrounding the site. The decrease of aerosol absorption coefficient from the midnight to the early morning (from 00:00 to 05:00 a.m.) suggests the removal by deposition of aerosol particles. A similar diurnal pattern for scattering coefficients was obtained, except that no significant peak around 08:00 a.m. was found corresponding to the local human activities. Consequently, the diurnal variation of SSA showed highest values in the afternoon with the maximum at around 14:00 p.m., and SSA decreased to the minimum observed at 07:00 a.m. This pattern of SSA diurnal variability indicated the enhancement of

ACPD
7, 13001–13033, 2007

light scattering aerosol loading during the afternoon, which might reflect the secondary aerosol production through the photochemical processes at the site. Both absorption and scattering coefficients measured at the SDZ site showed similar diurnal patterns as obtained at another GAW regional background station in the Yangtze delta region (Lin'An station in east part of china by Xu et al., 2002).

As previously discussed, the large value of S.D. for each of variables also indicated the strong day-to-day variations of aerosol optical properties measured at the site.

3.4 The aerosol optical properties with different air masses

In order to further understand the effects of different sources on aerosol optical properties, a trajectory clustering technique was applied in the analysis. In a cluster analysis, the root mean square deviations (RMS) for all trajectory segments were computed for each trajectory combination. The end points of the pair with the lowest RMS are then averaged together to obtain a new single average trajectory. The RMS of this average is then computed again for all trajectory combinations. This process continues until the global (all pairs) RMS deviation start to increase, at that point, only a few average trajectories are left (Stunder, 1996). In this work, we chose the January, February and December of 2004 to represent the winter period and the June, July and August of 2004 to represent the summer period.

Backward trajectories were calculated using an approach developed by Draxler (Draxler, 1997), and the meteorological data used were the NOAA/ARL archived reanalysis dataset (NOAA/ARL FNL dataset) with a time resolution of 6 h. Backward air mass trajectories were calculated for 36 h back in time at 100 m above the ground.

The cluster mean value of each parameter was calculated using the formula given below. It was composed of one-hour average data centered at each trajectory start time for all trajectories within that cluster:

$$\overline{A}_i = \frac{1}{n} \sum_j^n A_{i,j}, i = 1, N \quad (3)$$

where n represents the total number of trajectories in the ith cluster, $A_{i,j}$ represent the aerosol properties corresponding to the jth trajectory. N represents the total number of clusters.

Figure 5 shows the mean cluster trajectories to the site for the summer and winter periods, and Tables 6 and 7 present the cluster mean value of aerosol properties for each period respectively. For summer period, the cluster analysis had all trajectories grouped into 7 clusters (Fig. 5a). Trajectory clusters labeled #1, #2, and #6 were from the south sector of the site, and these air masses originated from the more heavily polluted regions. As Table 6 illustrates, cluster #1 was the most frequently observed flow pattern in the summer of the site, and the absorption and scattering coefficients of cluster #1 were quite high, with the mean values of 30.2 Mm^{-1} for absorption coefficient and 313.2 Mm^{-1} for scattering coefficient (see Table 6). A similar result was found for the cluster #2, for which the cluster mean absorption coefficient and scattering coefficients were 32.7 Mm^{-1} and 308.7 Mm^{-1} respectively. The SSA for both clusters had the same mean value of 0.89, which was the highest value among all the clusters, and also was higher than the SSA (0.81 and 0.793 respectively, see Table 3) reported for the Beijing urban areas (Bergin et al., 2001; Mao and Li, 2005). The 36-h average trajectory of cluster #1 and cluster #2 indicated that the air masses for both clusters were mainly from the heavily polluted regions. For instance, the average 36-h backward trajectory for cluster #1 could be traced back to Beijing and its southern outlying areas, and the average trajectory for cluster #2 extended longer distance (indicating more rapid transport) with the air masses passing through Beijing, Baoding, Shijiazhuang, and so on, which are all regions with large pollution emissions in northern China.

Cluster #6 represented the air masses coming from the south east directions. Along with the trajectory pathway, big industrial cities, such as Tianjin and Tangshan, were located within 200 km range from the site. Also the 36-h backward trajectory suggested that the air masses passed over the Shandong Peninsula (one of the rapidly developing regions in China) and could have come across the Bohai sea to influence the site. As a consequence, the mean absorption and scattering coefficient for cluster #6 were

ACPD
7, 13001–13033, 2007

the third highest among all the clusters, with the cluster mean absorption, scattering coefficient and SSA of 19.1 Mm^{-1}, 233.4 Mm^{-1}, and 0.89, respectively.

Cluster #3 was the second most frequently observed flow pattern to the site in the summer. The average 36-h backward trajectory of the cluster indicated the wind was weak and air masses for this cluster originated in the regions not far from the site because the pathway of the mean trajectory for this cluster was very short. The weak winds were ofterm observed during periods of stable atmospheric conditions, and in this case the site was influenced more by local sources and the accumulation of pollutants. The mean absorption and scattering coefficients were 19.0 Mm^{-1} and 117.5 Mm^{-1}, respectively, and the SSA was 0.84. The aerosol loading in the atmosphere for this cluster was lower than those with the air masses coming from the heavily polluted regions, such as cluster #1, #2 and #6, but was still rather high compared with those from the clean clusters, such as clusters #4, #5 and #7.

The clusters labeled #4, #5 and #7 represented the cases influenced by relatively clean air masses at the site according to the mean trajectory pathways (Fig. 5a) and the corresponding values of aerosol properties (see Table 6). The absorption and scattering coefficient were significantly lower than the previously discussed clusters, and the SSA for these three clusters ranged from 0.78 to 0.82, which were also significantly lower than the previously discussed clusters.

The above analysis showed the significant difference of aerosol properties among the clusters in summer period. The clusters with the trajectories passing through polluted regions had not only the higher absorption and scattering coefficients but also higher SSA values, while the clusters with mean trajectories passing through clean regions had lower absorption and scattering coefficient and lower SSA. This fact means that the aerosols coming from the polluted regions were more efficient at scattering light than those coming from clean regions during the summer period.

The average trajectory for each cluster in the winter period showed different flow patterns from those in summer. The trajectories were clustered into 10 groups in winter (Table 7). The number of trajectories for each cluster ranged from 20 to 40 except

ACPD
7, 13001–13033, 2007

for the cluster #10 (only four trajectories for SSA), and so in the following discussion the cluster #10 was not included. The pathway of air masses for cluster #1–#5 and #9 were from west and northwest directions, while the air masses for cluster #7 and cluster #8 were from southwest and west directions. According to the map of pollution source distributions indicated in Fig. 1, cluster #1–#5 and #9 mainly reflected the clean air sectors of the site, while cluster #7 and #8 indicated the polluted ones affected by air masses coming from the polluted regions. The cluster mean absorption and scattering coefficients given in Table 7 demonstrated that the measured results that were consistent with the pathways of air masses for each cluster (except for cluster #2), where low cluster mean absorption and scattering coefficients were found for clusters #1, #3, #4, #5, #9, while high absorption and scattering coefficients were observed for clusters #7 and #8. The pathway for cluster #2 was similar to that for cluster #3 although it passed slightly to the south of cluster #3 and showed slower transport. The cluster mean levels of absorption and scattering coefficients for trajectory cluster #2 were approximately twice as much as those of cluster #3, and a probable reason for this observation was because the air masses of this cluster were partly influenced by the emissions from the highly polluted city of Zhangjiakou and its surroundings. The pathway for cluster #6 was complicated, according to the average 36-h backward trajectory (Fig. 5b). The cluster mean trajectory shows air masses that originated from the clean regions in the northeast, and then passed through more polluted regions in the east and southeast, and the mixed influence of the clean and polluted air masses resulted in the relatively high level of aerosols at the site as given in Table 7.

Similar to the summer cases, the SSA values in winter were also relatively higher when the air masses were associated with the polluted pathways and relatively lower when the air masses were coming from the clean regions.

Filter sampling was conducted during subsets of the measurement period, and limited analyses of aerosol chemical composition and the corresponding aerosol optical properties are presented in Table 8. The filter samples were collected during the period from 17 July to 2 August 2004. Among the samples, the samples #6–#9 were

sampled on the "clean" days and the samples #1 and #2 on the polluted days. They represented the cases when the site influenced by polluted or clean air masses based on the calculated backward trajectories and the mass concentrations of each sample. Table 8 shows that sulfate, nitrate and ammonium accounted for about 70% or more of total PM2.1 (particles with aerodynamic diameter less than 2.1 μm) mass when the site was under polluted conditions, and less than 50% for the clean days. Moreover, the ratio of elemental carbon (light absorbing aerosol) to PM2.1 mass was relatively lower when the site was under polluted conditions. This analysis was consistent with the result from the trajectory clustering analysis that the air masses transport from polluted regions might increase the aerosol light scattering ability.

4 Conclusions

The means (S.D.) of scattering and absorption coefficients at a rural site in northern China for the entire measurement period were 174.6 Mm^{-1} (189.1 Mm^{-1}) and 17.5 Mm^{-1} (13.4 Mm^{-1}), respectively. The value was about one-third of reported value for scattering coefficient and about one-fifth of that for absorption coefficient obtained in the Beijing urban area. The mean SSA for the entire period was 0.88 (0.05), which was about 0.07 higher than the value reported by Bergin for Beijing urban area, and also higher than the value (0.85) in the climate model simulation for China and India. Both the absorption and scattering coefficients were lowest in winter (11.2 Mm^{-1} and 128.9 Mm^{-1}, respectively), while the highest values appeared in summer for absorption coefficient (22.1 Mm^{-1}) and in fall for scattering coefficient (208.2 Mm^{-1}). The mean SSA showed the lowest value in spring (0.85) and highest in winter (0.90).

The trajectory clustering analysis indicated that the scattering and absorption coefficients and SSA were all high when the air masses were coming from the densely populated and highly industrial areas. The SSA's associated with the polluted air masses were not only higher than those with the air masses coming from the "clean" directions, but also higher than the reported values measured at the pollution source regions,

ACPD
7, 13001–13033, 2007

this fact suggests that there may be substantial secondary aerosols production during the transport of air masses from the polluted regions. The aerosol optical properties measured at this rural area in northern China could server as reference material for radiative forcing estimations and regional climate modeling.

Acknowledgements. The authors thank the staffs of SDZ station for their cooperative woks during the experiment, and thank P. Sheridan of NOAA/CMDL for his kindly help in the preparation of the manuscript. This work was jointly supported by the China Ministry of Science and Technology Project No. 2001DIA10009, and the China NSF International Project No. 40121120827, and partly supported by the China NSF Project No. 40675009.

References

Akimoto, H. and Narita, H.: Distribution of SO2, NOx and CO2 emission from fuel combustion and industrial activities in Asia with 1°×1° resolution, Atmos. Environ., 28(2), 213–225, 1994.

Anderson, T. L., Masonis, S. J., Covert, D. S., Ahlquist, N. C., Howell, S. G., Clarke, A. D., and McNaughton, C. S.: Variability of aerosol optical properties derived from in situ aircraft measurements during ACE-Asia, J. Geophys. Res., 108(D23), 8647, doi:10.1029/2002JD003247, 2003.

Arnott, W. P., Hamasha, K., Moosmuller, H., Sheridan, P. J., and Ogren, J. A.: Towards aerosol light-absorption measurements with a 7-wavelength aethalometer: Evaluation with a photoacoustic instrument and 3-wavelength nephelometer, Aerosol Sci. Technol., 39, 17–29, 2005.

Arnott, W. P., Moosmuller, H., Sheridan, P. J., Ogren, J. A., Raspet, R., Slaton, W. V., Hand, J. L., Kreidenweis, S. M. and Collett, J. L.: Photoacoustic and filter-based ambient aerosol light absorption measurements: Instrument comparisons and the role of relative humidity, J. Geophys. Res., 108(D1), 4034, doi:10.1029/2002JD002165, 2003.

Barnard, J. C., Kassianov, E. I., Ackerman, T. P., Frey, S., Johnson, K., Zuberi, B., Molina, L. T., Molina, M. J., Gaffney, J. S., and Marle, N. A.: Measurements of Black Carbon Specific Absorption in the Mexico City Metropolitan Area during the MCMA 2003 Field Campaign, Atmos. Chem. Phys. Discuss., 5, 4083–4113, 2005, http://www.atmos-chem-phys-discuss.net/5/4083/2005/.

Bergin, M., Cass, G. R., Xu, J., Fang, F., Zeng, L. M., Yu, T., Salmon, L. G., Kiang, C. S., Tang, X. Y., Zhang, Y. H., and Chameides, W. L.: Aerosol radiative,physical, and chemical properties in Beijing During June 1999, J. Geophys. Res., 106(D16), 17 969–17 980, 2001.
Bodhaine, B. A.: Aerosol absorption measurements at Barrow, Mauna Loa and the South Pole, J. Geophys. Res., 100, 8967–8975, 1995.
Clarke, A. D. and Charlson, R. J.: Radiative Properties of the Background Aerosol: Absorption Component of Extinction, Science, 29, 263–267, 1985.
Cooke, W. F., Liousse, C., Cachier, H., and Feichter, J.: Construction of a 1°×1° fossil fuel emission data set for carbonaceous aerosol and implementation and radiative impact in the ECHAM4 model, J. Geophys. Res., 104, 22 137–22 162, 1999.
Delene, D. and Ogren, J. A.: Variability of aerosol optical properties at four North American surface monitoring sites, J. Atmos. Sci., 59(6), 1135–1150, 2002.
Draxler, R. R.: Description of the HYSPLIT-4 modeling system, NOAA Technical Memo., ERL ARL-224, 1997.
Dubovik, O., Holben, B. N., Eck, T. F., Smirnov, A., Kaufman, Y. J., King, M. D., Tanre, D., and Slutsker, I.: Variability of absorption and optical properties of key aerosol types observed in worldwide locations, J. Atmos. Sci., 59, 590–608, 2002.
Fuller, K. A., Malm, W. C., and Kredenweis, S. M.: Effects of mixing on extinction by carbonaceous particles, J. Geophys. Res., 104(D13), 15 941–15 954, 1999.
Hansen, A. D. A., Rosen, H., and Novakov, T.: The Aethalometer – an instrument for the real-time measurement of optical absorption by aerosol particles, Sci. Total Environ., 36, 191–196, 1984.
Holler, R., Ito, K., Tohno, S., and Kasahara, M.: Wavelength dependent aerosol single-scattering albedo: Measurements and model calculations for a coastal site near the Sea of Japan during ACE-Asia, J. Geophys. Res., 108, 8648, 2003.
Jacobson, M. Z.: Control of fossil-fuel particulate black carbon and organic matter, possibly the most effective method of slowing global warming, J. Geophys. Res., 107(D19), 4410, doi:10.1029/2001JD001376, 2002.
Man, C. K. and Shih, M. Y.: Light scattering and absorption properties of aerosol particles in Hong Kong, J. Aerosol Sci., 32, 795–804, 2001.
Mao, J. T. and Li, C. C.: Observational study of aerosol radiative properties over China. Acta Meteorologica Sinica, 63(5), 622–635. (in Chinese with English abstract), 2005.
Menon, S., Hansen, J., Nazarenko, L., and Luo, Y.: Climate Effects of Black Carbon Aerosols

in China and India, Science, 297, 2250–2253, 2002.
Moosmuller, H., Arnott, W. P., Rogers, C. F., Chow, J. C., Frazier, C. A., Sherman, L. E., and Dietrich, D. L.: Photoacoustic and filter measurements related to aerosol light absorption during the Northern Front Range Air Quality Study (Colorado 1996/1997), J. Geophys. Res., 103(D21), 28 149–28 157, 1998.
Ramanathan, V., Crutzen, P. J., and Kiehl, J. T. a. R. D.: Aerocols, Climate, and the Hydrological Cycle, Science, 294(5549), 2119–2124, 2001.
Rosenfeld, D.: TRMM observed first direct evidence of smoke from forest fires inhibiting rainfall, Geophys. Res. Lett., 26(20), 3105–3108, 1999.
Rosenfeld, D.: Suppression of rain and snow by urban and industrial air pollution, Science, 287, 1793–1796, 2000.
Schmid, O., Chand, D., and Andreae, M. O.: Aerosol Optical Properties in Urban Guangzhou, PRD workshop, Beijing, January 13–14, 2005.
Sheridan, P. J., Delene, D. J., and Ogren, J. A.: Four years of continuous surface aerosol measurements from the Department of Energy's Atmospheric Radiation Measurement Program Southern Great Plains Cloud and Radiation Testbed site, J. Geophys. Res., 106(D18), 20 735–20 747, 2001.
Street, D. G., Gupta, S., Waldhoff, S. T., Wang, M. Q., Bond, T. C., and Bo, Y.: Black carbon emission in China, Atmos. Environ., 35, 4281–4296, 2001.
Stunder, B. J. B.: An assessment of quality of forecast trajectories, J. Appl. Meteor., 35, 1313–1331, 1996.
Takemura, T., Nakajima, T., Dubovik, O., Holben, B. N., and Kinne, S.: Single scattering albedo and radiadive forcing of various aerosol species with a global three dimensional model, J. Climate, 15, 333–352, 2002.
Twomey, S.: The influence of pollution on the shortwave albedo of clouds. J. Atmos. Sci., 34, 1149–1152, 1977.
Weingartner, E., Saathoff, H., Schnaiter, M., Streit, N., Bitnar, B., and Baltensperger, U.: Absorption of light by soot particles: determination of the absorption coefficient by means of athalometer, J. Aerosol Sci., 34, 1445–1463, 2003.
Xu, J., Bergin, M. H., Greenwald, R., Schauer, J. J., Shafer, M. M., Jaffrezo, J. L., and Aymoz, G.: Aerosol chemical, physical, and radiaitve characteristics near a desert source region of northern China during ACE-Asia, J. Geophys. Res., 109, D19S03, doi:10.1029/2003JD004239, 2004.

Xu, J., Bergin, M. H., Yu, X., Liu, G., Zhao, J., Marrico, C. M., and Baumann, K.: Measurement of aerosol chemical, physical, and radiative properties in the Yangtze delta region of China, Atmos. Environ., 36, 161–173, 2002.
Yan, P., Zhang, Y., Yang, D., Tang, J., Yu, X., Cheng, H., Wang, S., Yu, X., Liu, G., and Zhou, X.: Characteristics of aerosol ionic compositions in summer of 2003 at Lin'An of Yangtze Delta Region, Acta Meteorologica Sinica, 20(3), 374–382, 2006.
Zhang, R., Xu, Y., and Han, Z.: Inorganic chemical composition and source signature of PM2.5 in Beijing during Ace-Asia period, Chinese Science Bulletin, 48(10), 1002–1005, 2003.

Table 1. The Measurements and instrumentations.

Measurements	Time period	Instrumentations
Scattering coefficientσ_{sc}	10 September 2003 to 15 January 2005	Integrating Nephelometer (Mode M9003, ECOTech, Australia), with wavelength of 520 nm
Absorption coefficientσ_{ab}	15 April 2003 to 15 January 2005	Aethalometer (Mode AE31, Magee Scientific, USA), with seven wavelength at 370, 470, 520, 590, 660, 880, 950 nm
Filter sampling for aerosol compositions (Ions and OC, EC)	Winter, 2 to 20 February 2004 Summer, 17 July to 2 August 2004	Andersen KA200 multi-stage impactors, with Quartz and Teflon sampling membrane

Table 2. The statistics results of 24 h average BC concentration, absorption and scattering coefficient and single scattering albedo SSA during the measurement at SDZ.

	BC Concentration (μg/m^3)	σ_{ab}Mm^{-1}	σ_{sc}Mm^{-1}	SSA
Mean	2.12	17.54	174.6	0.88
S.D.	1.62	13.44	189.1	0.05
Maximum	10.17	84.23	1381.8	0.97
Minimum	0.035	0.29	4.3	0.65
Median	1.78	14.71	101.6	0.90
Number of days	575	575	461	426

Table 3. Aerosol optical properties at some different regions.

Site	Period	σ_{ab}(Mm^{-1})	σ_{sc}(Mm^{-1})	SSA	References
SDZ, China (rural)	2003.9-2005.1	17.54	174.6	0.88	This work
Lin'an, China (rural)	1999.11	23	353	0.93	(Xu et al., 2002)
Yulin, China (Gobi desert)	2001.4	6	158	0.95	(Xu et al., 2004)
Cape D'Aguilar, Hongkong	1997.1–1998.2	25.72	64.77		(Man and Shih, 2001)
	1998.3–1998.4	15.79	38.65		
	1998.5–1998.8	6.03	8.71		
	1998.9–1998.10	18.98	70.91		
	1998.11–1999.2	31.22	96.75		
Beijing, China (urban)	1999.6	83	488	0.81	(Bergin et al., 2001)
Beijing, China (urban)	2003.6–12			0.793	(Mao and Li, 2005)
Bondville, Illinoise, US	1996.9.19–2000.9.26	4.66±2.27, <10 μm	57.7±17.7, <10 μm	0.924±0.0028, <10 μm	(Delene and Ogren, 2002)
Barrow,Alaska, US	1997.10.6-2000.9.26	0.39±0.41,<10 μm	9.76±5.20,<10 μm	0.99±0.48, <10 μm	
Southern Great Plain, US	1997.4.6-2000.9.26	2.46±1.09, <10 μm	46.9±16.9, <10 μm	0.947±0.025,<10 μm	

Table 4. The seasonal averages of absorption and scattering coefficient and SSA.

	σ_{ab}Mm^{-1})	σ_{sc}Mm^{-1}	SSA
Spring	19.89(13.75)	154.09(160.10)	0.85(0.05)
Summer	22.10(14.46)	190.30(167.52)	0.86(0.06)
Fall	15.11(11.26)	208.19(227.12)	0.89(0.05)
Winter	11.16(10.79)	128.92(150.93)	0.90(0.03)

Table 5. The number of days with fog and poor visibility in each month at SDZ.

Month	Fog/heavy fog (Day)	Visual range <10 km (Day)
Sep., 2003	13	14
Oct., 2003	4/1	12
Nov., 2003	11/2	13
Dec., 2003	1	1
Jan., 2004	1	1
Feb., 2004	2	1
March, 2004	4	4
April, 2004	5	4
May, 2004	4	4
June, 2004	4	3
July, 2004	12	10
Aug., 2004	8/1	8
Sep., 2004	12/1	12
Oct., 2004	8/2	10
Nov., 2004	6	5
Dec., 2004	5/2	4
Jan., 2005	3	7

Table 6. The mean optical properties for each cluster in summer (June, July and August, 2004).

Cluster No.	SSA	Number of trajectories	σ_{ab}Mm^{-1}	Number of trajectories	σ_{sc}Mm^{-1}	Number of trajectories
1	0.89(0.04)	106	30.24(15.93)	106	313.22(220.56)	116
2	0.89(0.05)	29	32.67(11.59)	29	308.66(159.49)	31
3	0.84(0.07)	80	18.97(10.69)	82	117.53(98.27)	90
4	0.78(0.08)	36	9.30(8.73)	39	32.56(33.38)	40
5	0.82(0.09)	29	10.11(6.28)	29	49.72(30.36)	29
6	0.89(0.06)	24	19.09(14.74)	24	233.36(200.68)	27
7	0.80(0.10)	17	12.17(10.26)	17	58.60(69.85)	24

Table 7. The mean optical properties for each cluster in winter (January, February and December, 2004).

Cluster No.	SSA	Number of trajectories	σ_{ab}Mm^{-1}	Number of trajectories	σ_{sc}Mm^{-1}	Number of trajectories
1	0.89(0.04)	36	3.65(2.74)	36	28.23(16.47)	36
2	0.88(0.05)	32	15.13(11.07)	34	126.21(104.59)	38
3	0.89(0.06)	20	7.24(7.50)	24	65.61(66.25)	20
4	0.90(0.04)	33	2.72(2.24)	35	22.93(15.39)	33
5	0.88(0.04)	30	4.38(4.04)	32	32.88(23.82)	33
6	0.91(0.04)	26	21.37(8.75)	33	281.81(173.50)	27
7	0.93(0.02)	24	34.66(11.93)	26	507.16(224.21)	27
8	0.91(0.03)	34	30.39(14.16)	35	375.66(271.10)	34
9	0.89(0.03)	20	2.93(1.59)	20	26.54(16.43)	21
10	0.88(0.04)	4	10.40(7.89)	4	71.09(53.23)	8

Table 8. The mass concentrations and percentage of selected chemical species in fine particles sampled during summer period at SDZ site.

Sample No.	Mass Conc. ($\mu g/m^3$)	NO_3^-	SO_4^{2-}	NH_4^+	OC	EC	Ions*/Mass (%)	EC/ Mass (%)	SSA
1 (polluted)	153.89	15.76	57.65	33.99	11.12	1.97	69.8	1.3	0.94
2 (polluted)	132.66	16.21	58.72	35.67	6.64	2.59	83.4	2.0	0.93
6 (clean)	32.79	4.85	7.15	4.24	4.61	0.89	49.5	2.71	0.87
7 (clean)	33.95	2.51	9.69	4.02	3.43	0.76	47.8	2.2	0.87
8 (clean)	12.84	0.14	3.20	1.02	1.58	0.29	34.0	2.2	0.83
9 (clean)	20.54	2.32	3.50	1.70	3.36	0.86	36.6	4.2	0.81

*Ions = (NO_3^- + SO_4^{2-} + NH_4^+)

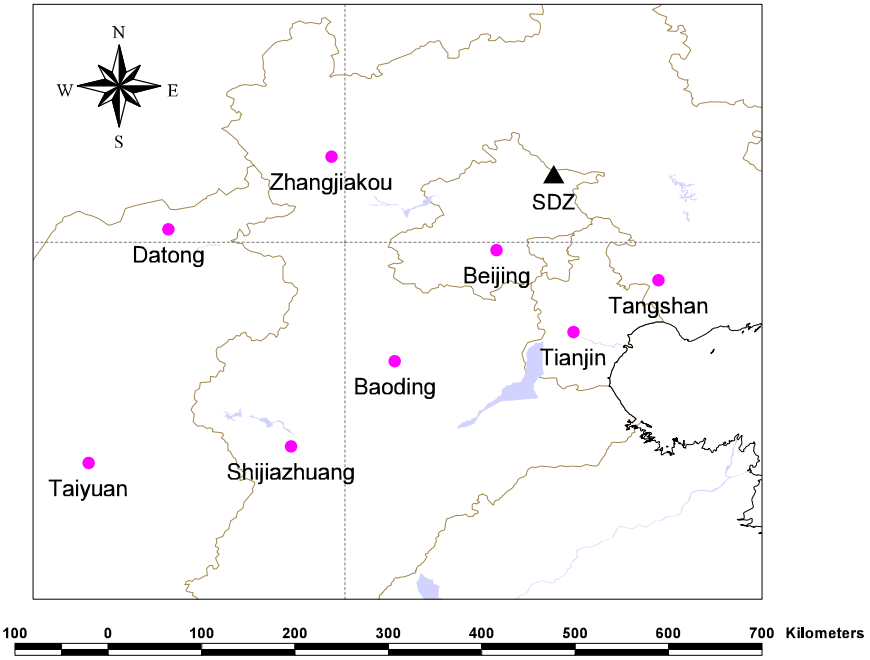

Fig. 1. Map of SDZ station and the major cities in the region.

ACPD
7, 13001–13033, 2007

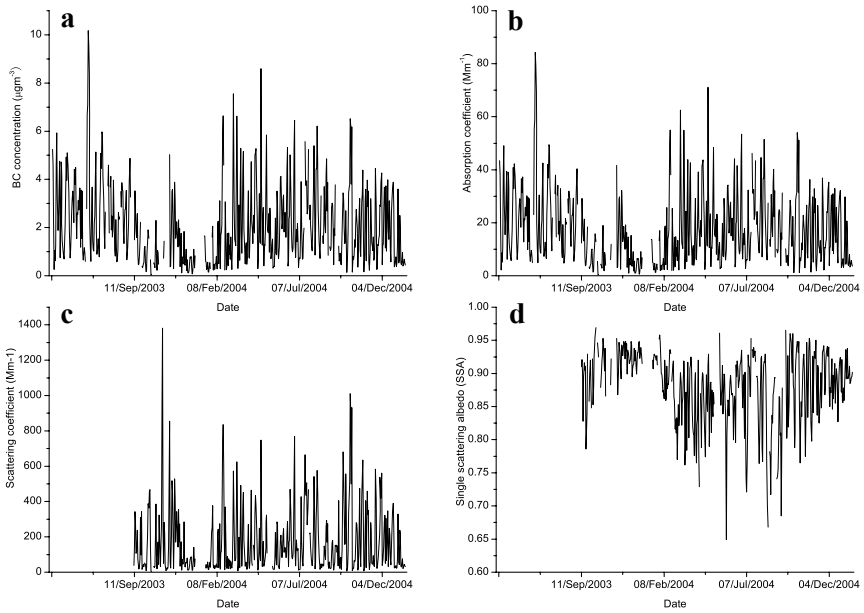

Fig. 2. The time series of daily averaged BC concentration, aerosol absorption and scattering coefficient, and single scattering albedo at SDZ **(a)** BC concentration, **(b)** Absorption coefficient, **(c)** Scattering coefficient, **(d)** Single scattering albedo (SSA).

ACPD
7, 13001–13033, 2007

EGU

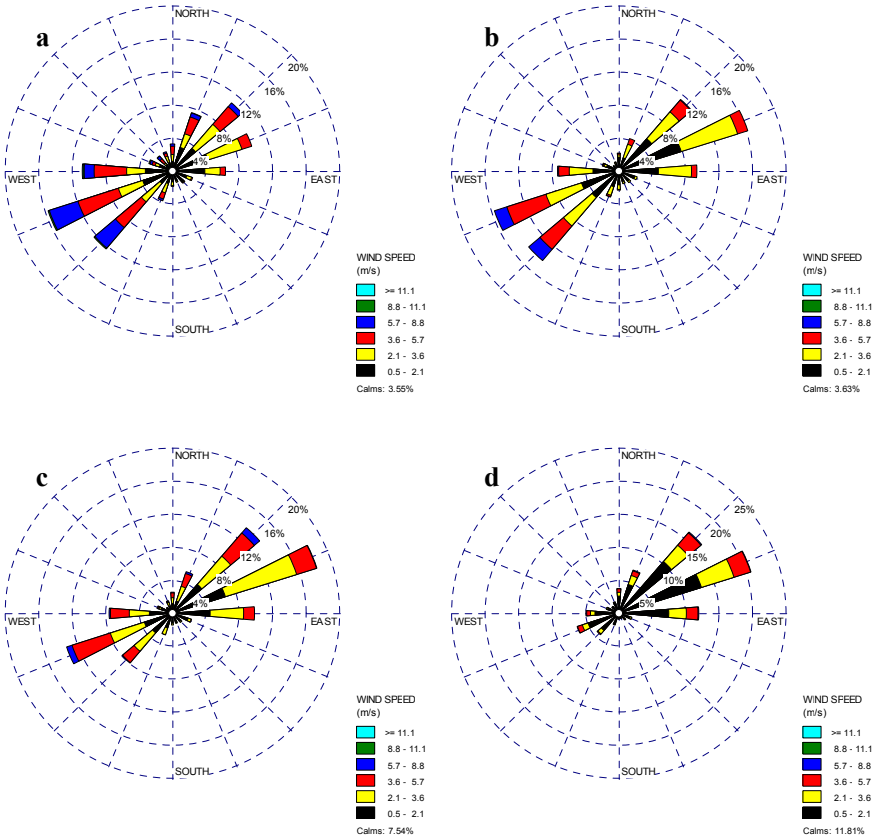

Fig. 3. Wind rose for surface wind at SDZ from Sept. 2003 to Jan. 2005 (plotted with WRPlot View software, http://www.weblakes.com/lakewrpl.html). **(a)** Spring, **(b)** Summer, **(c)** Fall, **(d)** Winter.

ACPD
7, 13001–13033, 2007

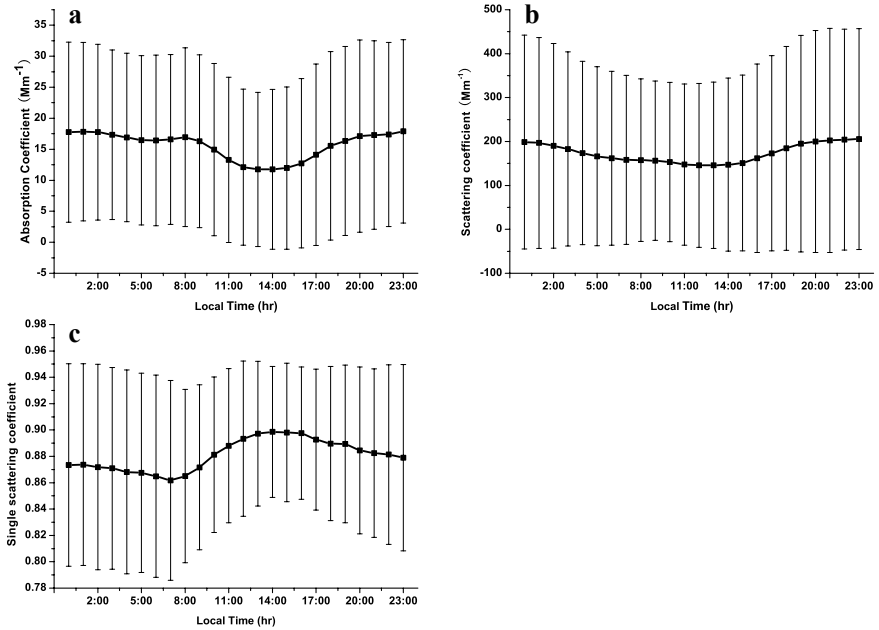

Fig. 4. Diurnal variability of aerosol optical properties at SDZ from September 2003 to January 2005, error bars represent S.D. **(a)** Absorption coefficient, **(b)** Scattering coefficient, **(c)** Single scattering albedo (SSA).

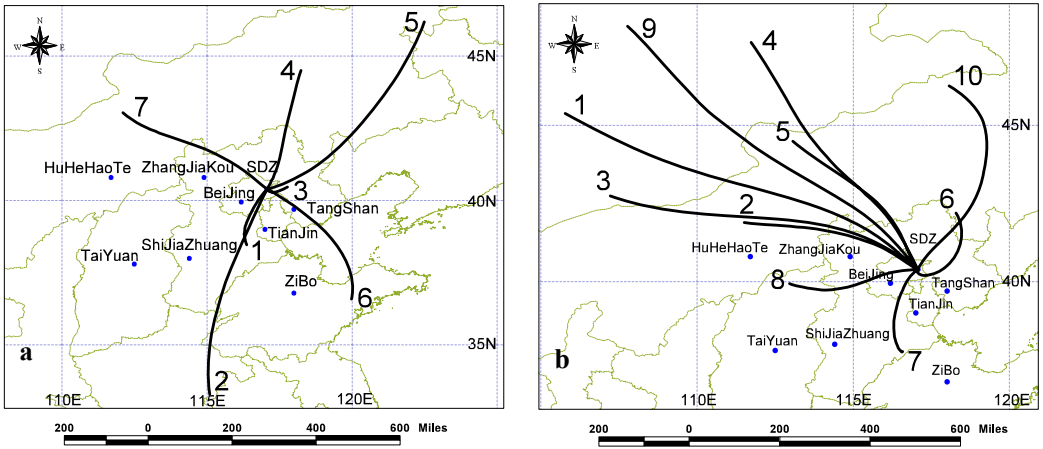

Fig. 5. The cluster mean 36 h backward trajectories for summer and winter periods at SDZ **(a)** Summer period (June, July, and Aug., 2004), **(b)** Winter period (Jan., Feb., and Dec., 2004).

ACPD
7, 13001–13033, 2007

EGU